JOURNAL OF SOLID STATE CHEMISTRY 35, 120–127 (1980)

Structure and "Oxidation Behavior" of $W_{24}O_{70}$, a New Member of the {103} *CS* Series of Tungsten Oxides

MARGARETA SUNDBERG

Department of Inorganic Chemistry, Arrhenius Laboratory, University of Stockholm, S-106 91 Stockholm, Sweden

Received April 13, 1979; in revised form January 2, 1980

Reduced tungsten trioxide crystals WO_{3-x}, formed by vapor transport from a preparation with bulk composition $WO_{\sim 2.90}$, have been studied by X-ray diffraction and electron microscopy. A single-crystal X-ray investigation showed the existence of the ordered {103} *CS*-structure $W_{24}O_{70}$, a new member of the homologous series W_nO_{3n-2}. Electron diffraction patterns of crystal fragments, with a few exceptions, showed the presence of the $W_{24}O_{70}$ phase (composition $WO_{2.917}$). Lattice images, however, indicated a fairly ordered {103} *CS*-phase, $W_{24}O_{70}$, intergrown with slabs of WO_3 giving gross compositions of the examined crystals in the range $WO_{2.93}$–$WO_{2.96}$. The wide WO_3 slabs were probably formed by an oxidation process during the preparation.

Introduction

In 1953, Magnéli introduced the concept "homologous series" (*1*) to denote slightly reduced structures of the ReO_3 type which contained "recurrent dislocations of atoms" along parallel planes, later called crystallographic shear (*CS*)-planes (*2*). At that time, $W_{20}O_{58}$ (*3*) was the only known member of the series Me_nO_{3n-2}. Figure 1 illustrates the structure of $W_{20}O_{58}$. The *CS*-planes run in the [$\bar{3}$01] direction of the parent WO_3 lattice and contain groups of six edge-sharing octahedra. Slabs of corner-sharing WO_6 octahedra (ReO_3 type), with a characteristic width equal to n, extend between the planes. The W atoms are all situated in a mirror plane perpendicular to the *CS*-planes.

Two additional members, $W_{25}O_{73}$ (*4*) and $W_{40}O_{118}$ (*5*), of the series have later been identified by X-ray methods. Both structures contain a puckered arrangement of the W atoms. Transmission electron microscopy observations of $W_{25}O_{73}$ crystals indicated some disorder in the *CS*-plane spacings. However, the average structure was found to be $W_{25}O_{73}$ (*4*).

Lately, electron microscopy observations of different samples of WO_{3-x}, $x \sim 0.1$, have shown that reduction of WO_3 to oxygen contents in the $0.07 \leq x \leq 0.12$ region introduces {103} *CS*-planes and yields structures corresponding to $W_{16}O_{46}$–$W_{30}O_{88}$ (*6–8*). Most of the examined crystals were formed under nonequilibrium conditions, which resulted in disorder in the spacings and in the directions of the {103} *CS*-planes, i.e., frequent twinning.

The present study was primarily initiated by the observation that needle crystals of a bulk composition $WO_{\sim 2.90}$ formed by vapor transport gave Weissenberg photographs which showed similarities to both $W_{20}O_{58}$ and WO_3. An investigation based upon X-ray data and transmission electron microscopy observations was carried out in order to clarify the detailed structure of a proba-

0022-4596/80/130120-08$02.00/0

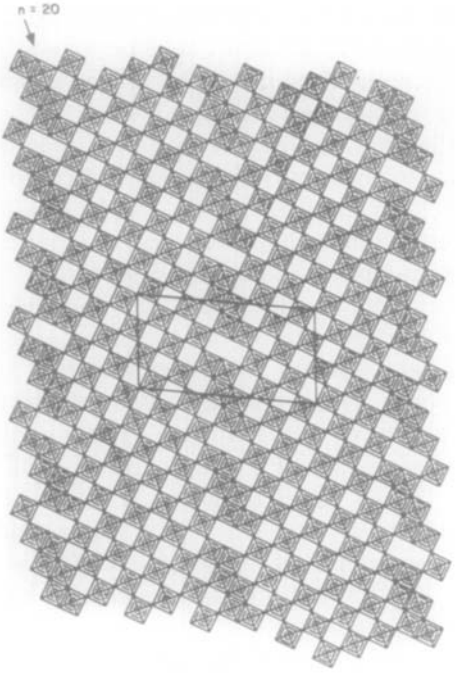

FIG. 1. Idealized representation of the monoclinic structure of $W_{20}O_{58}$ projected onto the *ac*-plane. The unit cell (of $W_{20}O_{58}$) is indicated. The number of octahedra in the diagonal row (arrow) between the *CS*-planes represents n in the formula W_nO_{3n-2}.

ble new member of the series W_nO_{3n-2}. Some preliminary data concerning this phase were presented by Magnéli (*9*).

Preparation

The following preparation method was originally planned as an attempt to prepare good-quality single crystals of $W_{20}O_{58}$. Amounts of WO_3 and WO_2 appropriate to give the gross composition $WO_{2.90}$ were carefully mixed and then heated in evacuated sealed silica tubes for 10 days in a moderate temperature gradient (~75°C). The sample ($WO_{2.90}$) was kept in the hotter part of the furnace, T = 1075°C, while the crystals examined in this study formed in the cooler part of the sample tube (1000°C). The temperatures were maintained for 3 days, and then lowered by 175°C over 3 days and again held fixed for 4 days (cooler end at 825°C). Finally, the sample was quenched to room temperature. The amount of transported material formed was too small for chemical analysis.

Optical microscopy showed the residue to consist of tiny dark-blue needles, while the transported part contained fairly large dark-blue needles of different lengths. The Guinier powder photograph of the residue indicated the phase $W_{20}O_{58}$ (*3*) and was not further considered. The Guinier photograph of the transported crystals indicated a phase mixture of {103} *CS*-structure and WO_3(*o*-rh.).

Single-Crystal X-Ray Investigation

Several different transported crystals were examined by the Weissenberg technique. After a long exposure time a rotation photograph showed that the *b*-axis length was 7.56 Å, twice that of $W_{20}O_{58}$ (*3*), giving rise to weak extra layer lines. The Weissenberg photographs indicated that the reflection positions in the reciprocal lattice planes *h*0*l*, *h*2*l*, and *h*4*l* were practically identical and similar to those of $W_{20}O_{58}$. The positions of the reflections, all very weak, in the *h*1*l* and *h*3*l* reciprocal lattice planes were identical, and in addition these layer lines were somewhat similar to the weak layer lines of WO_3 (mon.) with l = odd. The weak reflections gave rise to a doubling of the *a*- and *b*-axes and hence a superstructure. The diffraction spots were mostly very streaked in the *c*-axis direction, indicating disorder in the structure. The unit cell dimensions of the subcell were found to be a = 12.07 Å, b = 3.78 Å, c = 28.9 Å, β = 98.6°. A Patterson projection based on data from the *h*0*l* reciprocal lattice plane (Fig. 2) could be interpreted in terms of a structure $W_{24}O_{70}$, homologous to that of $W_{20}O_{58}$ (*3*).

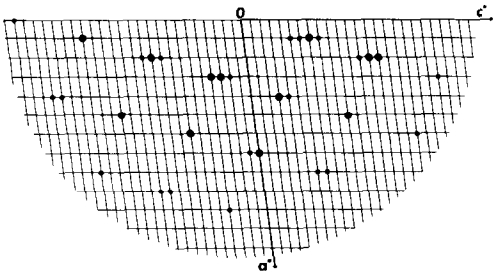

FIG. 2. The reciprocal lattice plane *h0l* (the planes *h2l* and *h4l* look essentially the same). Lattice points corresponding to observed reflections are marked with dots.

Electron Microscopy Investigation

Transported crystals were also examined by transmission electron microscopy using the lattice image technique described, for example, by Iijima (*10*), and by Allpress and Sanders (*11*). The crystals were crushed under *n*-butanol in an agate mortar and deposited on a perforated carbon film supported by a copper grid. Then the crystal fragments were examined in a Siemens ELMISKOP 102 equipped with a double tilt-lift stage and operated at 125 kV. Only very thin crystal fragments extending across holes in the carbon film were examined. They were aligned with the electron beam parallel to the short crystal *b*-axis, so that the (*h0l*) section could be viewed on the screen. The size of the objective aperture used corresponded to 0.27 $Å^{-1}$.

Electron diffraction patterns recorded from some 25 crystal fragments showed all flakes to contain {103} *CS*-planes. The electron diffraction spots were also more or less streaked, indicating disorder in the flakes (Fig. 3). In a few cases the *n* value could not be exactly calculated because of severe streaking, and sometimes two sets of spots corresponding to two different *n* values were superimposed. The distribution of evaluated *n* values from 24 different crystal flakes is shown in Fig. 4. The dominating value is $n = 24$, suggesting a composition close to $W_{24}O_{70}$ ($WO_{2.917}$) of the transported crystal fragments being studied.

Lattice images of the same crystal fragments in most cases showed regions of fairly well-ordered *CS*-plane spacings, separated by wide slabs of apparently unreduced WO_3. Examples are given in Figs. 5a and b, which show the micrographs of two different crystal fragments. Figure 5a depicts a fairly well-ordered crystal fragment, while the one in Fig. 5b is much more disordered. The *CS*-plane spacings were carefully measured and the corresponding *n* values calculated. Figure 6a shows the distribution of *CS*-plane spacings over a region

FIG. 3. Electron diffraction pattern taken of a transported crystal fragment with $n \sim 24$. The diffraction spots are somewhat streaked which indicates disorder.

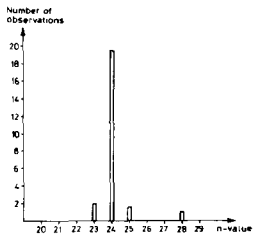

FIG. 4. The distribution of *n* values evaluated from 24 different crystal fragments. *n* corresponds to the spacing in the ordered structure of W_nO_{3n-2}. The dominating *n* value is $n = 24$. When the diffraction pattern indicated two different *n*-values a weight of $\frac{1}{2}$ was assigned to each.

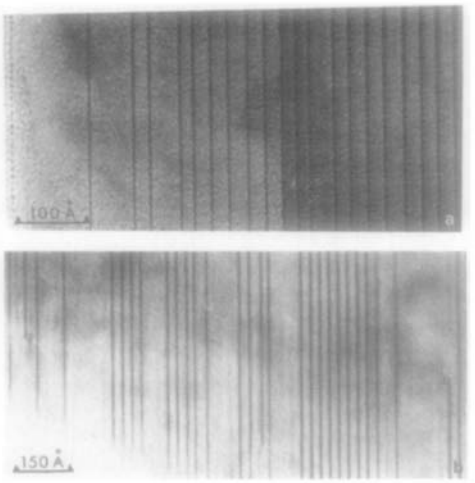

FIG. 5. Lattice images of two transported crystal fragments. (a) A fairly well-ordered crystal fragment with three large *CS*-plane spacings is shown. (b) Lattice image of transported crystal fragment $WO_{\sim 2.95}$ showing the *CS*-phase $W_{24}O_{70}$ intergrown with slabs of apparently unreduced WO_3 (giving an overall composition $WO_{\sim 2.95}$). Stopping and weak traces of *CS*-planes can be seen.

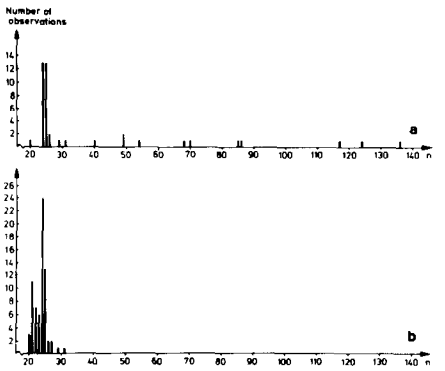

FIG. 6. (a) Distribution of *CS*-plane spacings evaluated from the flake shown in Fig. 5b. The *x*-axis represents the width of the *CS*-plane spacings, expressed by the corresponding *n* value, while the *y*-axis gives the frequency. (b) Distribution of *CS*-plane spacings evaluated from the same fragment as in Fig. 5b, but after introduction of hypothetic *CS*-planes.

of ~1900 Å in the same crystal as in Fig. 5b. The variation in spacing over a group of *CS*-planes is in the range 23–37 Å, corresponding to n = 20–31. From the distribution of *CS*-plane spacings the composition of the crystal fragment was calculated to be $\sim WO_{2.95}$.

More statistical evidence was obtained when the images of seven different crystal fragments were analyzed. The results are shown in Table I. The interplanar spacing varied within the range 21–38 Å over a group of *CS*-planes, corresponding to n = 18–32, with a pronounced maximum at n = 24. The widths of the large *CS*-free slabs

TABLE I

AVERAGE COMPOSITION OF SEVEN CRYSTAL FRAGMENTS BEFORE AND AFTER INTRODUCTION OF HYPOTHETIC *CS*-PLANES

Diffraction pattern n	Variation in width over a group of *CS*-plane spacings: Range n	Variation in width over a group of *CS*-plane spacings: Mode n	Average composition of the studied crystal fragments WO_x	Average composition of the flake after introduction of hypothetic *CS*-planes: WO_x	Average composition of the flake after introduction of hypothetic *CS*-planes: n
24	18–32	25	2.941	2.917	24
25	22–32	24, 25	2.935	2.920	25
24	20–31	24, 25	2.949	2.917	24
24	19–32	24, 25	2.949	2.917	24
24	23–31	24	2.951	2.917	24
25	19–29	25	2.938	2.913	23
23	18–30	23	2.952	2.913	23

were mostly in the region 50–160 Å. Some larger spacings have also been observed. The average composition WO_x of the crystal fragments studied seems to be in the region $x = 2.93$–2.95.

An observation frequently made is illustrated in Fig. 5b. At some places in the wide *CS*-free slabs, stopping *CS*-planes and weak contrast feature resembling diffuse shear planes can be seen. This observation initiated a careful examination of the wide WO_3 bands. It turned out that hypothetic *CS*-planes could be inserted in the wide WO_3 slabs in such a way that a uniform *CS*-plane spacing was obtained. The results are shown in Table I. As an example, if such an insertion is made in Fig. 5b the histogram of Fig. 6a will turn into that of Fig. 6b. The *CS*-plane spacings will now be distributed over the region 23–37 Å, corresponding to $n = 20$–31, with a maximum at $n = 24$, giving the average composition $\sim WO_{2.917}$ of the flake. This agrees with the value $n = 24$ obtained from the corresponding electron diffraction pattern.

Discussion

The results obtained from diffraction experiments, both the electron diffraction study (shown in Fig. 3) and the single-crystal X-ray investigation, indicate that the dominating structure is $W_{24}O_{70}$; hence the composition $WO_{2.917}$ (apart from some disorder) of the examined crystal fragments. On the other hand, the results obtained from the lattice images show an entirely different composition of the fragments. Still, however, the crystal structure seems to be the *CS*-phase $W_{24}O_{70}$, intergrown with slabs of apparently unreduced WO_3 to give an overall composition in the region $WO_{2.93}$–$WO_{2.96}$.

The $W_{24}O_{70}$ crystal structure is very similar to that of $W_{20}O_{58}$, shown in Fig. 1. The main difference is that the $W_{24}O_{70}$ slabs are 24 octahedra wide in the characteristic direction instead of 20 as in $W_{20}O_{58}$. Another difference between the two oxides concerns the positions of the tungsten atoms. In $W_{20}O_{58}$ all W atoms are located at the plane $y = 0.5$ (3) but in "$W_{24}O_{70}$," the W atoms are displaced from that plane. It was not possible to solve the displacement of W atoms from the center of the octahedra in detail from the X-ray data, but the observation of weak reflections in odd reciprocal lattice planes suggested an arrangement of the W atoms similar to that in WO_3 (mon. or *o*-rh.). In WO_3 (mon.) (*12*) there is a three-dimensional displacement of the W atoms from the center of the octahedra, while in WO_3 (*o*-rh.) (*13*) the displacement is only in two directions. Both these types of displacement are shown in Fig. 7.

Earlier X-ray investigations of {103} *CS*-structures have shown that $W_{25}O_{73}$ and $W_{40}O_{118}$ have puckered arrangements of the W atoms (*4*, *5*) whereas $W_{20}O_{58}$ has not. In $W_{25}O_{73}$, the displacement of the W atoms in the *b*-axis direction is least at the *CS*-plane and is largest in the middle of the slab (*4*).

As discussed above the crystals examined consisted of a {103} *CS*-structure $\sim W_{24}O_{70}$ intergrown with slabs of unreduced WO_3. The fact that WO_3 is the substructure of the shear structure, is the reason why the X-ray investigation did not reveal the bands of *CS*-free tungsten trioxide. However, the weak reflections in the

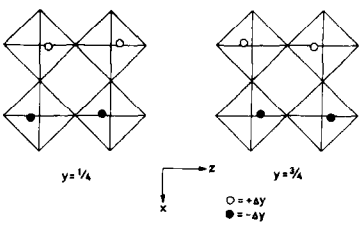

FIG. 7. Displacements (exaggerated) of the W atoms from the centers of the octahedra are shown for WO_3 (mon.). In the WO_3 (*o*-rh.) structure the displacements are essentially the same in the *y*- and z-direction but with no displacement in the *x*-direction.

odd reciprocal lattice layers, which cause the doubling of the crystal b-axis and hence a superstructure similar to that of WO_3 (mon. or o-rh.), may be caused largely by the displacements of the W atoms in the wide WO_3 slabs.

Another observation, which is important in the discussion of the type of displacement of the W atoms in different tungsten oxides, is the length of the corresponding unit cell b-axis. Magnéli *et al.* (*15*) pointed out that the length of the b-axis in the $(Mo,W)_nO_{3n-1}$ series decreases with increasing tungsten content, reflecting the formation of more regular WO_6 octahedra. From Table II, which shows the unit cell dimensions of different tungsten oxides, it can be seen that the oxides $W_{25}O_{73}$ and $W_{40}O_{118}$ have b-axes > 3.8 Å. These two oxides adopt puckered arrangements of the tungsten atoms. The crystals examined in this study have a b-axis which is about the same length as that in WO_3 (mon.) and WO_3 (o-rh.) and also very close to that of $W_{20}O_{58}$ (apart from the doubling). This fact probably indicates that the examined crystals do not have strongly one-dimensionally puckered arrangements of the W atoms such as those in $W_{25}O_{73}$ and $W_{40}O_{118}$.

According to earlier studies of the formation and growth of *CS*-planes in reduced WO_3 (*16*) some *CS*-planes in Fig. 8 can be interpreted as having grown into crystal during observation in the electron microscope. This *in situ* reduction which sometimes took place was due to the high vacuum in the electron microscope in combination with the heat from the electron beam (*16*). The new *CS*-planes were mostly observed to grow between existing planes, in the *CS*-region. If a new *CS*-plane grew in the WO_3 slab, the growth always took place at the edge close to existing *CS*-planes—never in the middle of the slab, as can be seen in Fig. 8. This observation probably indicates that the off-center displacement of W atoms decreases from a maximum in the wide WO_3 slab to a minimum at the *CS*-planes. It seems likely that the displacements of W atoms in the wide

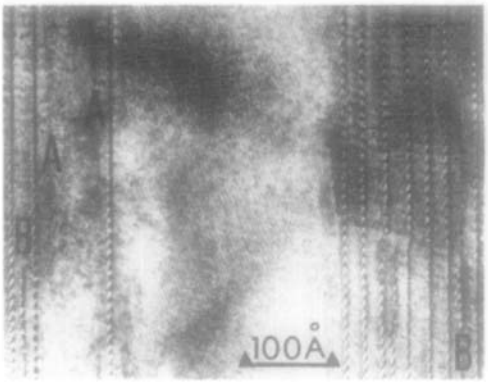

FIG. 8. Groups of fairly well-ordered *CS*-phase W_nO_{3n-2} slabs intergrown with slabs of apparently unreduced WO_3 can be seen. Weak traces of probably "old" *CS*-planes can be seen at A. Traces of *CS*-planes formed in the electron microscope can be seen at B.

TABLE II

UNIT CELL DIMENSIONS OF TUNGSTEN OXIDES

	a (Å)	b (Å)	c (Å)	β	Reference
$W_{20}O_{58}$	12.05	3.767	23.59	94.72°	(*3*)
$\sim W_{24}O_{70} + WO_3$	24.1	7.54	28.9	98.6°	This study
$W_{25}O_{73}$	11.93	3.82	59.72	98.3°	(*4*)
$W_{40}O_{118}$	11.9	3.815	49.4	106.4°	(*5*)
WO_3 (mon.)	7.30	7.53	7.68	90.54°	(*12*)
WO_3 (o-rh.)	7.341	7.57	7.754		(*13*)
WO_3 (tetr.)	5.25		3.91		(*14*)

WO_3 slab are larger than those in the *CS*-regions. A large displacement of W atoms thus probably stabilizes the local composition of the apparently unreduced WO_3 domains.

The above observation also agrees with the postulation that the growth of new *CS*-planes is controlled by the elastic strain energy (*17*). Theoretical calculations on similar situations (*18–20*) have shown that this factor could be important in this sort of situation.

The observation of stopping *CS*-planes and weak traces of *CS*-planes in wide WO_3 slabs may indicate that the sample has been oxidized in the course of the preparation, after the formation of a shear structure. As can be seen from the last column in Table I, the introduction of hypothetic *CS*-planes in wide WO_3 slabs reduced the composition of the studied crystal flakes to within the region $WO_{2.913}$–$WO_{2.926}$, with an average composition of the sample at $WO_{2.917}$ (n = 24). This value of the composition agrees too well with results obtained from the X-ray study and the electron diffraction pattern to be pure coincidence.

Another interesting fact is that the average oxygen content of the crystal fragments studied ($WO_{2.93}$–$WO_{2.96}$) is higher than expected for a material containing {103} *CS*-planes. In previous electron microscopy observations of slightly reduced tungsten trioxide {103} *CS*-planes have only been observed for compositions up to $\sim WO_{2.93}$ (*6–8*). Above $\sim WO_{2.93}$ {102} *CS*-planes have been found (*7, 21, 22*).

The observations suggested the following hypothesis for the formation of the wide *CS*-plane spacings. The transported crystals were originally formed with an overall composition W_nO_{3n-2}, $n \sim 24$ (in accordance with the electron diffraction pattern and the X-ray observations). Decreasing temperature during the experiment caused a change of the equilibrium in the sample tube toward more oxidizing conditions, which resulted in elimination of some *CS*-planes. The oxidation of the *CS*-planes did not take place uniformly through the examined crystal fragments, but was concentrated to some parts of the crystals where it resulted in a locally complete reoxidation of the flake.

A systematic variation of the *CS*-spacings within the "$W_{24}O_{70}$" regions, similar to what has been reported for slightly reduced rutile (*23*), has not been observed. This is consistent with the hypothesis that an oxidation with elimination of shear planes in wide areas has taken place.

It is interesting to note that the wide slabs of unreduced WO_3 have been found in several samples of vapor-grown crystals containing {103} *CS*-planes, but never in the bulk material.

From the results presented here, concerning transported crystals of slightly reduced tungsten trioxide, it can be seen that the composition is not the only relevant factor influencing the shear type. The formation of wide *CS*-plane spacings which probably takes place by an oxidation process during the preparation is still not solved in detail, but further experiments are under way which hopefully will clarify the oxidation mechanism. The investigation illustrates also the complementary applicability of the X-ray and electron microscopy techniques. The X-ray study gave detailed information about the idealized atomic arrangement of the $W_{24}O_{70}$ phase. The presence of WO_3 intergrown with the $W_{24}O_{70}$ phase could only be found by means of the lattice image investigation.

Acknowledgments

I wish to express my thanks to Professor Arne Magnéli and Dr. Lars Kihlborg for their interest and many stimulating discussions throughout the work. The present study has been performed within a research program supported by the Swedish Natural Science Research Council.

References

1. A. MAGNÉLI, *Acta Crystallogr.* **6,** 495 (1953).
2. A. D. WADSLEY, *Rev. Pure Appl. Chem.* **5,** 165 (1955).
3. A. MAGNÉLI, *Ark. Kemi* **1,** 513 (1950).
4. M. SUNDBERG, *Acta Crystallogr. B* **32,** 2144 (1976).
5. P. GADÓ AND A. MAGNÉLI, *Acta Chem. Scand.* **19,** 1514 (1965).
6. J. G. ALLPRESS AND P. GADÓ, *Cryst. Lattice Defects* **1,** 331 (1970).
7. M. SUNDBERG AND R. J. D. TILLEY, *J. Solid State Chem.* **11,** 150 (1974).
8. R. PICKERING AND R. J. D. TILLEY, *J. Solid State Chem.* **16,** 247 (1976).
9. A. MAGNÉLI, *React. Solids Proc. Int. Symp. 8th 1976* (1977).
10. S. IIJIMA, *Acta Crystallogr. A* **29,** 18 (1973).
11. J. G. ALLPRESS AND J. V. SANDERS, *J. Appl. Crystallogr.* **6,** 165 (1973).
12. L. KIHLBORG, unpublished results.
13. E. SALJE, *Acta Crystallogr. B* **33,** 574 (1977).
14. W. L. KEHL, R. G. HAY AND D. WAHL, *J. Appl. Phys.* **23,** 212 (1952).
15. A. MAGNÉLI, B. BLOMBERG-HANSSON, L. KIHLBORG, AND G. SUNDKVIST, *Acta Chem. Scand.* **9,** 1382 (1955).
16. M. SUNDBERG AND R. J. D. TILLEY, *Phys. Status Solidi A* **22,** 677 (1974).
17. S. IIJIMA, *J. Solid State Chem.* **14,** 52 (1975).
18. E. IGUCHI AND R. J. D. TILLEY, *Phil. Trans. Roy. Soc. London Ser. A* **286,** 55 (1977).
19. E. IGUCHI AND R. J. D. TILLEY, *J. Solid State Chem.* **24,** 121 (1978).
20. E. IGUCHI AND R. J. D. TILLEY, *J. Solid State Chem.* **24,** 131 (1978).
21. R. J. D. TILLEY, *Mater. Res. Bull.* **5,** 813 (1970).
22. J. G. ALLPRESS, R. J. D. TILLEY, AND M. J. SIENKO, *J. Solid State Chem.* **3,** 440 (1971).
23. L. A. BURSILL AND B. G. HYDE, *Phil. Mag.* **23,** 3 (1971).